Do Large Effect QTL Fractionate? A Case Study at the Maize Domestication QTL *teosinte branched1*

Anthony J. Studer[1] and John F. Doebley
Department of Genetics, University of Wisconsin, Madison, Wisconsin 53706

ABSTRACT Quantitative trait loci (QTL) mapping is a valuable tool for studying the genetic architecture of trait variation. Despite the large number of QTL studies reported in the literature, the identified QTL are rarely mapped to the underlying genes and it is usually unclear whether a QTL corresponds to one or multiple linked genes. Similarly, when QTL for several traits colocalize, it is usually unclear whether this is due to the pleiotropic action of a single gene or multiple linked genes, each affecting one trait. The domestication gene *teosinte branched1* (*tb1*) was previously identified as a major domestication QTL with large effects on the differences in plant and ear architecture between maize and teosinte. Here we present the results of two experiments that were performed to determine whether the single gene *tb1* explains all trait variation for its genomic region or whether the domestication QTL at *tb1* fractionates into multiple linked QTL. For traits measuring plant architecture, we detected only one QTL per trait and these QTL all mapped to *tb1*. These results indicate that *tb1* is the sole gene for plant architecture traits that segregates in our QTL mapping populations. For most traits related to ear morphology, we detected multiple QTL per trait in the *tb1* genomic region, including a large effect QTL at *tb1* itself plus one or two additional linked QTL. *tb1* is epistatic to two of these additional QTL for ear traits. Overall, these results provide examples for both a major QTL that maps to a single gene, as well as a case in which a QTL fractionates into multiple linked QTL.

QUANTITATIVE trait loci (QTL) mapping studies have become widely used to elucidate the genetic architecture of trait variation in many organisms (Mackay *et al.* 2009). A common observation in these studies is that QTL of large effect are often detected. Noor *et al.* (2001) have questioned whether such large effect QTL represent single genes or groups of tightly linked genes. These authors have suggested that such large effect QTL, upon closer examination, might fractionate into multiple linked small effect QTL, representing multiple genes. A single QTL does not necessarily equal a single gene. Even in cases where QTL effects have been fine mapped to a specific gene, the research may not formally exclude the presence of additional linked genes that contribute to the overall QTL effect for that genomic region.

Doebley and Stec (1991, 1993) identified a QTL of large effect on the long arm of maize chromosome 1, controlling the differences in plant and ear architecture between maize and teosinte. These authors proposed that *tb1*, a known mutant of maize, was the gene underlying this QTL because *tb1* falls within the 1 LOD support interval for the QTL, and because the *tb1* mutant and the QTL affect the same suite of traits. Subsequently, Doebley *et al.* (1995) used a complementation test that showed that the teosinte allele of the QTL fails to complement the *tb1* mutant of maize, indicating that they are alleles of the same gene. However, complementation tests do not provide formal proof because of the potential for nonallelic noncomplementation.

Additional support for the hypothesis that *tb1* is the gene underlying the major domestication QTL was obtained after the cloning of *tb1* (Doebley *et al.* 1997). With knowledge of the molecular identity of *tb1*, Doebley *et al.* (1997) showed that the maize allele of this gene is expressed at twice the level of the teosinte allele in the developing branch and in immature ears. Thus, a change in gene regulation was hypothesized to be the causative difference between maize and teosinte. Finally, Clark *et al.* (2006) provided formal proof that *tb1* is the QTL by fine mapping the QTL to a 12-kb "control region" located ~58–69 kb upstream of the *tb1* open reading frame. These authors further demonstrated that this control region contains a factor that acts as a *cis*-regulatory

doi: 10.1534/genetics.111.126508
Manuscript received January 5, 2011; accepted for publication April 4, 2011
Supporting information is available online at http://www.genetics.org/cgi/content/full/genetics.111.126508/DC1.
[1]Corresponding author: Department of Genetics, University of Wisconsin, 425 Henry Mall Genetics/Biotech Bldg. 5210, Madison, WI 53706. E-mail: studer@wisc.edu

element with the maize allele conditioning a higher level of *tb1* expression than the teosinte allele. However, their data do not address the possibility of additional QTL linked to *tb1*, and indeed some of their data suggest that such additional linked QTL may exist, *i.e.*, that *tb1* fractionates into multiple linked QTL.

In this article, we report two experiments performed to address whether there are additional QTL closely linked to *tb1*. In experiment I, we analyzed a mapping population in which the *tb1* control region identified by Clark *et al.* (2006) is fixed for the teosinte haplotype, but the regions flanking it are segregating for maize *vs.* teosinte chromosomal segments. If there are additional QTL linked to the control region, then there should be phenotypic effects associated with the segregating maize *vs.* teosinte chromosomal segments, despite the fact that the *tb1* control region is not segregating. Conversely, if the control region alone explains all phenotypic effects, then there should be no phenotypic effects associated with the flanking chromosomal regions. In experiment II, we analyzed a set of nearly isogenic recombinant inbred lines (NIRILs) for the *tb1* genomic region to see whether we could detect any QTL other than *tb1*. This experiment has more power than a standard QTL analysis to detect closely linked QTL because the NIRILs have an isogenic background and the NIRILs were grown in replicate to obtain better estimates of QTL effects.

On the basis of these two experiments, we confirm that *tb1* is a large effect QTL contributing to the differences in plant and ear architecture between maize and teosinte. In fact, *tb1* is the only QTL for plant architecture traits that we detected. However, we identify four additional QTL affecting ear architecture. One of these additional QTL is located only 6 cM upstream of *tb1*. Two of these additional QTL have significant epistatic interactions with *tb1*. Thus, our results provide examples for both a major QTL that maps to a single gene as shown for plant architecture, as well as a case in which a QTL fractionates into multiple QTL as shown for ear architecture.

Materials and Methods

Plant materials

Segments of the long arm of chromosome 1 from teosinte were introgressed into a maize inbred W22 background for both experiments I and II. For experiment I, a segment of the long arm of chromosome 1 from a teosinte (*Zea mays* ssp. *mexicana*; collection Wilkes-Panindicuaro) was introgressed into W22 via six generations of backcrossing (Figure 1). A BC_6S_1 line (I01) that was homozygous for the teosinte alleles at markers *bnlg615* and *bnlg1671*, which flank *tb1*, was recovered. I01 was then crossed to W22 and the F_2 progeny of this cross were screened for crossovers near *tb1*. A plant with one of the newly identified recombinants was itself crossed to W22, and the F_2 progeny of this cross were screened for crossovers near *tb1*. From this process, a homozygous introgression line (I16) containing an ~69-kb segment of teosinte chromosome that encompasses the *tb1* upstream control region and part of the ORF was recovered (Clark *et al.* 2006). Homozygous I01 and I16 lines were crossed and the resulting F_1 plants were selfed to produce an F_2 population for experiment I.

For experiment II, a segment of the long arm of chromosome 1 (T1L) from a teosinte (*Z. mays* ssp. *parviglumis*; Iltis and Cochrane collection 81) was introgressed into W22 via six generations of backcrossing (Figure 1). During the backcrossing process, molecular markers were used both to follow the target segment surrounding the QTL on the long arm of chromosome 1, as well as to eliminate teosinte chromosome segments at other major domestication QTL identified by Doebley and Stec (1993) (supporting information, Table S1). Six separate BC_6 plants heterozygous for the target segment were selfed to give six BC_6S_1 families (designated families A–E). These six families were selfed an additional five generations to produce a set of 153 homozygous NIRILs. These 153 lines were distributed among the six families as follows: A, 24; B, 31; C, 39; D, 25; E, 19; and F, 15. These lines possess a set of maize–teosinte recombinant chromosomes for the *tb1* genomic region in the W22 genetic background. These 153 lines make up the QTL mapping population of experiment II.

Molecular markers and linkage map

Plants in experiment I were genotyped using a PCR-based indel marker, GS3, previously described by Clark *et al.* (2006). GS3 is located in the coding region of *tb1* and segregates in the I01 × I16 F_2 population. Plants in experiment II were genotyped using a set of 25 PCR-based markers: 16 SSRs, six insertion or deletion (indel), and three markers scored for the presence/absence of a PCR product (Figure 3). Marker information is available at either Panzea (www.panzea.org) or MaizeGDB (www.maizegdb.org). There were a total 174 crossovers among the 153 lines, averaging 1.1 crossovers per line. The distribution of crossovers among lines was as follows: 0 (46 lines), 1 (52 lines), 2 (44 lines), 3 (10 lines), and 4 (1 line). A genetic map was constructed using the Kosambi map function and a genotyping error rate of 0.0001 as parameter values for the "est.map" command in the R/qtl module of the R statistical computing package (Broman *et al.* 2003).

Phenotypic data collection

The plants for experiment I were grown at the University of Wisconsin West Madison Agricultural Research Station, Madison, WI, during summer 2006. F_2 seed from three ears (A, B, and C) generated by three separate I01 × I16 crosses was planted in a randomized complete block design using a grid with 0.9-m spacing between plants in both dimensions. This spacing minimized the degree to which plants shaded their neighbors. The following five traits were phenotyped for experiment I: cupules per rank (CUPR) (number of cupules in a single rank from base to the tip of the ear), ear diameter (ED) (diameter, in millimeters, of the

midsection of each ear), lateral branch internode length (LBIL) (mean internode length, in centimeters, of the uppermost lateral branch), tillering (TILL) (the ratio of the sum of tiller heights/plant height), and tiller number (TILN) (the number of tillers per plant). CUPR and ED were both measured on the uppermost, well-formed lateral inflorescence (ear) of each plant.

The NIRILs for experiment II, along with the backcross parent W22, were grown using a randomized complete block design at the University of Wisconsin West Madison Agricultural Research Station during summer 2008. The design included three replicates (blocks A, B, and C) with a single 10-plant plot of each NIRIL per replicate. Each plot was 3.7 m long and 0.9 m wide. The plots within each block were arranged in a grid with row and column designations so that position effects could be included during data analysis. Three plants were phenotyped per plot. In addition to the five traits measured in experiment I, the following three traits were evaluated: 10-kernel length (10KL) (length, in millimeters, of 10 consecutive kernels in a single rank along the ear), ear length (EL) (distance, in centimeters, from the base to the tip of the ear), and percent staminate spikelets (STAM) (percentage of male spikelets in the inflorescence). 10KL, CUPR, ED, EL, and STAM were all measured on the uppermost, well-formed lateral inflorescence (ear) of each plant.

Data analysis

For experiment I, we used the GLM procedure of SAS (Littel *et al.* 1996) to compare the effects of the I01 and I16 introgression segments on phenotypes. Genotype (homozygous I01, homozygous I16, or heterozygous) and ear parent (A, B, or C) were considered as fixed effects. The general linear model used was

$$Y_{ijk} = \mu + a_i + b_j + e_{ijk}$$

,where Y_{ijk} is the trait value for the *kth* plant from the *jth* ear parent with *ith* genotype, μ is the overall mean of the experiment, a_i is the genotype effect, b_j is the ear parent effect, and e_{ijk} is the sampling error. Using this model, the effects of the different introgressions (I01 *vs.* I16) were evaluated.

For experiment II, we obtained least-squares means for each NIRIL using the MIXED procedure of SAS (Littel *et al.* 1996). The NIRIL (or parental) lines and families (A–E) were considered fixed effects while blocks (A, B, and C) and plot coordinates were treated as random effects. The linear model used was

$$Y_{hijklm} = \mu + a_h(b_i) + b_i + c_j + d_k + f_l + e_{hijkl} + g_{hijklm},$$

where Y_{hijklm} is the trait value for the *mth* plant at *lth* column and *kth* row in the *jth* block of the *hth* NIRIL nested in the *ith* family, μ is the overall mean of the experiment, a_h is the NIRIL (or parental) line effect, b_i is the family effect, c_j is the block effect, d_k is the row effect, f_l is the column effect, and e_{hijkl} is the experimental error (random variation among plots), and g_{hijklm} is the (within-plot) sampling error. All fixed effects were significant and were included in the model for the calculation of the least-squares means. The random effects of this full model were subjected to the likelihood ratio test for significance for each trait. Effects that were not significant were dropped from the model on a trait-by-trait basis.

The least-squares means estimates were used for QTL mapping in experiment II, which was conducted in the R/qtl module of the R statistical computing package (Broman *et al.* 2003). For each trait, an initial QTL scan was performed using simple interval mapping with a 0.25-cM step (Lander and Botstein 1989) and the position of the highest LOD score was recorded. Statistical significance of the peak LOD score was assessed using 10,000 permutations of the data (Doerge and Churchill 1996). Then, the position and effect of the QTL was refined using the Haley–Knott regression method (Haley and Knott 1992) by executing the "calc.genoprob" command (0.25-cM step size and assumed genotyping error rate of 0.001), followed by the "fitqtl" command. To search for additional QTL, the "addqtl" command was used. If a second QTL was detected, then fitqtl was used to test a model containing both QTL and their interaction effect. If both QTL remained significant, the "refineqtl" command was used to reestimate the QTL positions on the basis of the full model including both QTL. Finally, each QTL was removed from the model and then added back using the addqtl command to reconfirm its significance and position. Approximate confidence intervals for the locations of the QTL were obtained via 1.5 LOD support intervals to each side of the position of the LOD maximum.

We calculated broadsense heritabilities (H^2) for experiment II on a line mean basis

$$H^2 = \frac{\sigma_g^2}{\sigma_g^2 + \sigma_{ge}^2 + \left(\sigma_e^2\right)/r}$$

where σ_g^2 is the genotypic variance, σ_{ge}^2 is the genotype × environment interaction variance, and σ_e^2 is the experimental error variance divided by the number of replicates ($r = 9$). We used the MIXED procedure of SAS to fit a linear random-effect model for the estimation of the variance components (Littel *et al.* 1996). All data for both experiments 1 and 2 are available at www.panzea.org.

Results

Experiment I

To test whether the *tb1* control region identified by Clark *et al.* (2006) is sufficient to explain all of the phenotypic effects observed when a teosinte segment of the long arm of chromosome 1 is introgressed into W22, we analyzed an F_2 family from an I01 (full introgression segment) × I16 (*tb1* control region only) cross (Figure 1). A general linear model was used to compare the effects among the genotypic classes in this family (Table 1). For plant architecture (branching) traits (LBIL, TILL, and TILN), we could not reject the null

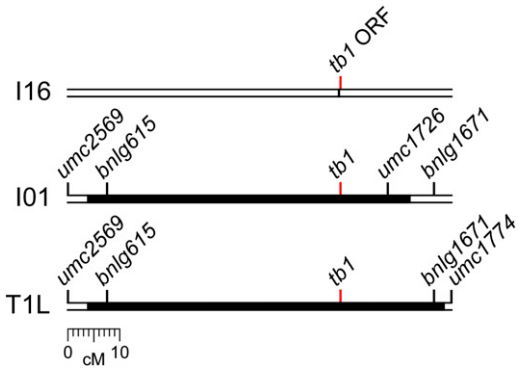

Figure 1 Map of the introgression lines used. All introgressed segments are drawn to scale. Solid areas indicate teosinte chromosome segments; open areas represent maize chromosome segments. Markers flanking the introgressions and the position of *tb1* are shown for reference. The introgressed segment in I16 is only ~69 kb.

hypothesis that I01 and I16 have equal effects on phenotype, indicating that there are no additional QTL for these traits beyond the control region identified by Clark *et al.* (2006). However, for ear morphology traits (CUPR and ED), I01 and I16 have significantly different phenotypic effects. Thus, there must be QTL in addition to the *tb1* control region for ear traits.

Experiment II

Quantitative trait variation: Given that experiment I indicated that there are one or more ear trait QTL linked to the *tb1* control region, we attempted to map these QTL using a set of 153 NIRILs in experiment II. These lines were grown in a randomized block design with three blocks and one plot of each line per block. The least-squares means for each trait for each NIRIL were estimated using a mixed linear model. The heritabilities of the traits are generally high with all values being >0.7 (Figure 2).

Histograms of the trait distributions show a large degree of separation between the phenotypic means for the two parental lines for all traits except EL (Figure 2). For example, for TILN, the maize parent has a mean value of ~0.5 tillers, while the teosinte parent has a value of 2 tillers. For all traits, the mean values for the maize parental line was located toward the edge of the trait distributions representing more maize-like phenotypes, while the mean values for the teosinte parental line was associated with more teosinte-like phenotypes. The trait distributions tend to be somewhat bimodal and/or skewed (Figure 2). 10KL has a distinctly bimodal distribution while other traits are more weakly bimodal (CUPR, LBIL, and TILL). For traits with a bimodal distribution, the means for the maize and teosinte parental lines are each located at one of the two modes of the distribution. In all cases the trait distributions are skewed toward teosinte-like phenotypic values. This skew toward teosinte-like phenotypes occurs due to the excess of NIRILs with the maize genotype in the NIRIL population. For example, 44 NIRILs were recovered that genotyped maize at all 25 markers, whereas only 2 NIRILs were recovered that genotyped teosinte throughout the region.

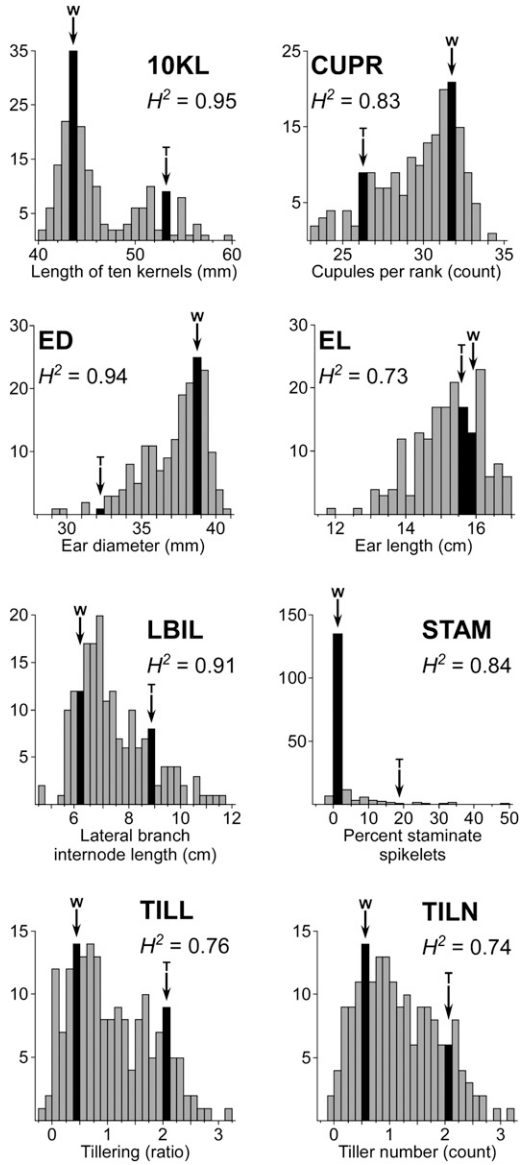

Figure 2 Frequency distribution of nearly isogenic recombinant inbred lines (NIRILs) least-squares means of the eight traits measured in this study. The arrows and solid bars indicate the bin containing the parental lines: maize inbred W22 (W) and introgression line W22-T1L (T). Heritabilities were calculated on a plot basis for each trait. Traits are abbreviated as follows: 10-kernel length (10KL, in millimeters), cupules per rank (CUPR), ear diameter (ED, in centimeters), ear length (EL, in centimeters), lateral branch internode length (LBIL, in centimeters), staminate spikelets (STAM, percent), tillering (TILL), and tiller number (TILN).

Table 1 Experiment I results: the comparison of introgressed segment I01 to I16

Trait	Additive effects	*P*-value	Units
CUPR	−1.1044	<0.0001	Count
ED	−1.7403	<0.0001	mm
LBIL	−0.0620	0.4600	cm
TILL	0.0042	0.9344	Ratio
TILN	−0.0612	0.2402	Count

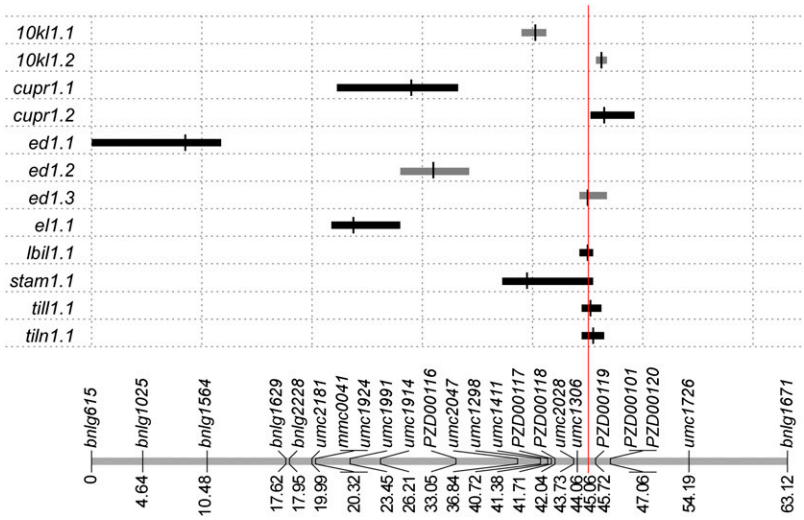

Figure 3 Map of the 12 QTL detected in this study on chromosome arm 1L. Horizontal bars for each QTL represent the 1.5-LOD support interval and the narrow vertical line marks the position of the peak LOD score: black bars indicate additive QTL and gray bars indicate QTL with interactions. The red line marks the position of *tb1*. QTL names are based upon the trait name abbreviations followed by the chromosome number; the numbers after the period enumerate the QTL detected for each trait. Traits are abbreviated as in Figure 2. The genetic map below the QTL plot indicates the extent of the introgressed W22-T1L segment. The position of each marker locus is shown in centimorgans.

EL is the one trait for which the maize and teosinte parental lines are the least differentiated (Figure 2). This is because ear length is a composite of two other traits—the number of kernels or cupules along the length of the ear (CUPR) and the length of each cupule or kernel (10KL). For CUPR, the maize parent line has a larger number of cupules (kernels) than the teosinte parent line, contributing to a longer ear relative to teosinte. However for 10KL, the maize parent line has less elongated cupules, giving it a shorter ear relative to teosinte. Thus, overall the maize and teosinte parent lines have ears that are roughly equivalent in length but with different underlying morphological bases.

QTL mapping: We identified 12 QTL for the eight traits in the 63.1-cM region on chromosome 1 (Figure 3, Table 2). The LOD thresholds ($P = 0.01$) for QTL detection were between 2.42 and 2.58, depending on the trait. All 12 QTL have associated LOD scores of ≥5.5, thus they have strong statistical support. For five of the eight traits (EL, LBIL, STAM, TILL, and TILN), a single QTL was detected, while for three traits (10KL, CUPR, and ED) two or more QTL were detected. Significant interaction effects were also detected for the two QTL controlling 10KL and ED. The R^2 values for the genetic models for the traits range from 0.15 to 0.88. In most cases, the model R^2 values correspond closely to the H^2 values. For example, R^2 *vs.* H^2 are 0.88 *vs.* 0.95 for 10KL, 0.69 *vs.* 0.83 for CUPR, 0.73 *vs.* 0.94 for ED, and 0.70 *vs.* 0.76 for TILL. This correspondence indicates that the detected QTL and interactions explain all or most of the heritable variation among the NIRILs.

Single QTL were identified for five of the eight traits analyzed: EL, LBIL, STAM, TILL, and TILN. Four of the five single QTL (*lbil1.1*, *stam1.1*, *till1.1*, and *tiln1.1*) have 1.5-LOD intervals that include *tb1* (Figure 3). The QTL for EL (*el1.1)* is located 21 cM upstream of *tb1*and its 1.5-LOD support interval is well separated from *tb1*. The single QTL at *tb1* for LBIL, TILL, and TILN all have relatively large effects with large R^2 and H^2 values (Table 2, Figure 3). The position and effect of *lbil1.1*, *till1.1*, and *tiln1.1* suggest that *tb1* explains all or most of the genetic variation for these traits. These three large effect single QTL over *tb1* all pertain to plant architecture traits. The remaining five traits are not governed by a single QTL at *tb1* and these five traits are all ear traits. These results indicate that large effect QTL at *tb1* accounts for all of the variation for plant traits among these lines, although ear traits have a more complex genetic architecture. These results are consistent with the results of experiment I.

Multiple QTL were identified for 10KL, CUPR, and ED (Table 2, Figure 3). In all cases, the multiple QTL for a single trait act in the same direction with the maize alleles contributing to a maize-like phenotype and the teosinte alleles to a teosinte-like phenotype. For two traits (10KL and ED), significant interaction effects were identified between QTL. For all traits with multiple QTL, the QTL with the largest LOD score for each trait had a 1.5-LOD interval that includes, or is <1 cM away from, *tb1*. For example, *ed1.3*, which falls directly over *tb1*, has a large LOD score (22.5), while the other two QTL for ED have much smaller LOD scores (10.1 and 9.3). Thus, these data suggest that *tb1* is the major QTL for 10KL, CUPR, and ED, even if there are other QTL within the introgressed segment.

Refining QTL positions: For 10KL and CUPR, the largest effect QTL falls near *tb1* but *tb1* lies outside the 1.5-LOD support interval. Since there are two QTL for each of these traits, we reassessed whether the presence of multiple QTL was biasing the estimates of the QTL positions. We subdivided the dataset to fix one of the QTL for a single genotype (maize or teosinte) and then scanned the segregating region that remained for QTL. By scanning for QTL with these subsets of the data, we can reevaluate whether there are two QTL in the positions indicated by our initial analysis.

For *10kl1.1*, two subsets of the data were analyzed: lines fixed for the maize allele of *10kl1.2*, and lines fixed for the teosinte allele of *10kl1.2*. When *10kl1.2* is fixed for the

Table 2 Experiment II results: QTL summary data

QTL	Position (cM)	LOD score	CI (cM)	Additive effect	Units	LOD cutoff	R^2	H^2
10kl1.1	40.25	24.9	39.00–41.25	3.5	mm		13.5	
10kl1.2	46.25	26.1	45.75–46.75	6.0	mm		14.5	
10kl1.1:2		9.8		6.6	mm		4.2	
10KL_Model		70.1		16.1	mm	2.58	87.9	0.95
cupr1.1	29.00	6.5	22.50–33.25	−1.7	Count		6.8	
cupr1.2	46.50	26.3	45.25–49.25	−3.5	Count		38.1	
CUPR_Model		38.4		−5.2	Count	2.51	68.5	0.83
ed1.1	8.50	9.3	0.00–11.75	−1.7	mm		8.8	
ed1.2	31.00	10.1	28.00–34.25	−1.4	mm		9.7	
ed1.3	45.00	22.5	44.25–46.75	−2.7	mm		26.5	
ED1.2:3		5.2		−2.4	mm		4.6	
ED_Model		43.1		−8.2	mm	2.45	72.7	0.94
el1.1	23.75	5.5	21.75–28.00	−0.8	cm	2.45	15.3	0.73
lbil1.1	45.00	36.5	44.25–45.50	2.4	cm	2.42	66.7	0.91
stam1.1	39.50	13.6	37.25–45.50	10	Percent	2.45	31.5	0.84
till1.1	45.25	40.2	44.50–46.25	1.3	Ratio	2.56	70.2	0.76
tiln1.1	45.50	37.1	44.50–46.50	1.2	Count	2.42	67.2	0.74

teosinte allele, *10kl1.1* is still detected and in the same position (Table 3). When *10kl1.2* is fixed for the maize allele, *10kl1.1* is not detected. This result was not unexpected because of the large interaction term between *10kl1.1* and *10kl1.2*. These results indicate that *10kl1.1* is real but only has an effect on phenotype when the teosinte allele is present at *10kl1.2* due to an epistatic interaction. Thus, *10kl1.2* is epistatic to *10kl1.1*. This epistatic interaction is plainly visible when the mean 10KL values for the different two-locus genotypic classes are compared (Figure 4A).

For *10kl1.2*, two subsets of the data were analyzed: lines fixed for the maize allele at *10kl1.1* and lines fixed for the teosinte allele at *10kl1.1*. When *10kl1.1* is fixed for the teosinte allele, *10kl1.2* is still detected and in the same position (Table 3). When *10kl1.1* is fixed for the maize allele, *10kl1.2* is still detected but it is shifted in position to fall over *tb1*. Thus, the presence of *10kl1.2* is confirmed, and this analysis shows that the effects are independent of the allelic composition at *10kl1.1*. However, the conflicting results on its position indicate some uncertainty about its exact location. One possibility is that *10kl1.2* is located at *tb1*.

For *cupr1.1*, two subsets of the data were analyzed: lines fixed for the maize allele of *cupr1.2* and lines fixed for the teosinte allele of *cupr1.2*. When *cupr1.2* is fixed for the teosinte allele, *cupr1.1* is still detected but it is shifted in position to be over *ed1.2* (Table 3). When *cupr1.2* is fixed for the maize allele, *cupr1.1* is not detected. This result was not surprising because an interaction term between *cupr1.1* and *cupr1.2* was nearly significant in the original analysis (*P*-value of 0.0106 with a 0.01 cutoff). These results indicate that *cupr1.1* is real but only has an effect on phenotype when the teosinte allele is present at *cupr1.2* because of an epistatic interaction between these two QTL. This epistatic interaction is plainly visible when the mean CUPR values for the different two-locus genotypic classes are compared (Figure 4B).

For *cupr1.2*, two subsets of the data were analyzed: lines fixed for the maize allele at *cupr1.1* and lines fixed for the teosinte allele at *cupr1.1*. When *cupr1.1* is fixed for the teosinte allele, *cupr1.2* is still detected and it is located in the same position (Table 3). When *cupr1.1* is fixed for the maize allele, *cupr1.2* is still detected but it is shifted in position to fall over *tb1*. Thus, the presence of *cupr1.2* is confirmed, and this analysis shows that the effects are independent of the allelic composition at *cupr1.1*. However, the conflicting results on its position indicate some uncertainty about its exact location. One possibility is that *cupr1.2* is located at *tb1*.

We also reassessed the position of *stam1.1*. The 1.5-LOD interval for this QTL includes *tb1*; however, the maximum LOD is located near *10kl1.1*. We evaluated whether a model

Table 3 Experiment II reanalysis: refined QTL positions

QTL	Fixedmarker	Refined position (cM)	Original position (cM)	LOD score	Refined CI (cM)	Original CI (cM)
10kl1.1	*PZD00119*-T	40.38	40.25	10.0	38.64–41.48	39.00–41.25
10kl1.1	*PZD00119*-M	—	40.25	—	—	39.00–41.25
10kl1.2	*umc1298*-T	46.23	46.25	9.2	45.73–46.93	45.75–46.75
10kl1.2	*umc1298*-M	45.37	46.25	11.0	42.24–51.63	45.75–46.75
cupr1.1	*PZD00119*-T	30.56	29.00	4.1	25.16–35.33	22.50–33.25
cupr1.1	*PZD00119*-M	—	29.00	—	—	22.50–33.25
cupr1.2	*umc1914*-T	48.99	46.50	12.8	45.79–51.78	45.25–49.25
cupr1.2	*umc1914*-M	46.18	46.50	18.9	44.43–49.20	45.25–49.25

M, maize allele; T, teosinte allele. LOD scores obtained with a subset of the full data in which one of the two QTL affecting the trait was fixed for a single genotype.

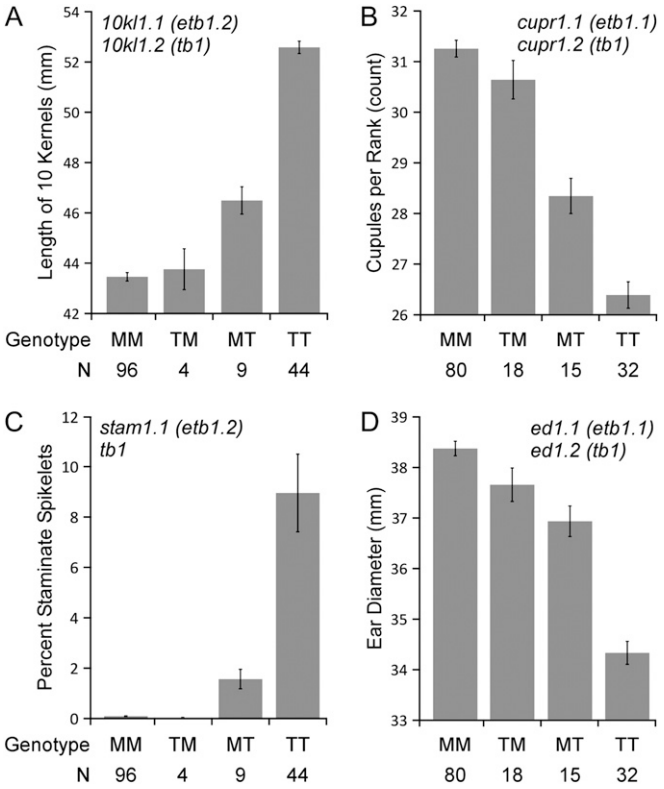

Figure 4 Mean phenotypic values of four genotypic classes. The *x* axis denotes the number of line representing each genotypic class (N) and the alleles (maize, M; teosinte, T) for the closest marker to the QTL effecting the trait and *tb1*, respectively. A and C's (*etb1.2*) closest marker is *umc1298*. B and D's (*etb1.1*) closest marker is *PZD00116*. Eight of the 153 lines had missing data for *PZD00116* and were not included. Error bars represent the standard error for each genotypic class. Traits are abbreviated as in Figure 2.

involving two linked QTL for STAM would best explain the data. Since *tb1* was expected to affect STAM on the basis of the known effects of the *tb1* mutant allele (Doebley *et al.* 1997), we considered a model with one QTL at *tb1* and a second QTL at the position of the LOD maximum for *stam1.1*. The original analysis may have failed to define two separate QTL because of their proximity to one another. We examined the mean values for STAM of the four genotypic combinations of *stam1.1* and *tb1* (Figure 4C). From this figure, *stam1.1* only has an effect on phenotype when there is a teosinte allele at *tb1*. However, *tb1* has a strong effect on phenotype whether *stam1.1* is fixed for the maize or the teosinte allele. The highest value for STAM is obtained when there are teosinte alleles at both *tb1* and *stam1.1*. These results suggest that there are two QTL interacting to control STAM: *stam1.1* with an effect that is dependent on the teosinte allele at *tb1* and *tb1* with an effect regardless of the genotype of *stam1.1*. Thus, *tb1* is epistatic to *stam1.1*.

Discussion

Clark *et al.* (2006) studied how an ~54-cM teosinte chromosome segment encompassing the *tb1* gene affected plant and ear architecture when it was introgressed into maize inbred W22. Their analyses enabled them to map a factor controlling these phenotypes to a region between ~58 and 69 kb upstream of the *tb1* open reading frame. Their experiments demonstrated that this control region has strong effects on phenotypes, but they did not formally exclude the possibility that there are other linked QTL in the introgressed teosinte chromosome segment.

A closer examination of the results by Clark *et al.* (2006) suggests that there may be other QTL linked to *tb1*. Their results do indicate the *tb1* control region explains all effects on plant architecture. For example, their full ~54-cM (~59 Mbp) introgression segment (I01) has effects on plant architecture that are indistinguishable from those of a partial <1-cM introgression containing only ~69 kb surrounding the *tb1* control region (I16). However, for traits related to ear architecture, their results appear more complex. For example, their smaller introgression (I16) appears to have a weaker effect on CUPR than their full ~54-cM introgression. In general, their introgression lines containing larger segments of the teosinte genome appear to have stronger effects on ear traits (CUPR and 10KL) than their introgression lines possessing smaller introgressed segments that are shortened on either the proximal or distal side of the *tb1* control region. These observations suggest that there are additional QTL linked to *tb1* with effects on ear traits. However, due to their experimental design, a direct comparison of introgressed segments could not be made.

To determine whether there are additional QTL for plant and ear architecture linked to *tb1*, we performed an experiment (experiment I) to test whether a minimal introgression of the *tb1* control region (I16) was sufficient to produce the same phenotypes as a full introgression segment (I01) that extended both proximal and distal to *tb1*. The results of experiment I showed no difference among the genotypic classes in the F_2 population derived from the I01 × I16 cross for plant architecture phenotypes (LBIL, TILL, and TILN). This result indicates that the control region identified by Clark *et al.* (2006) is the only QTL for plant architecture located in the introgressed chromosome segment. However, the three genotypic classes in the F_2 population did differ from one another for the ear morphology phenotypes (ED and 10KL). Thus, experiment I indicates that there are additional QTL linked to the *tb1* control region that affect ear morphology.

To map these additional QTL, a second experiment (experiment II) was done using a set of NIRILs. These lines contained recombinant chromosomes with cross-overs throughout the region, giving us the ability to map QTL to relatively small intervals. The replicated design of the experiment gave relatively high heritabilities for the traits, providing power to detect QTL with modest effects. Because our study used lines that are isogenic except for the ~63-cM region surrounding *tb1*, there were no QTL segregating in other regions of the genome that could complicate our ability to detect QTL near *tb1*. The analysis of these NIRILs

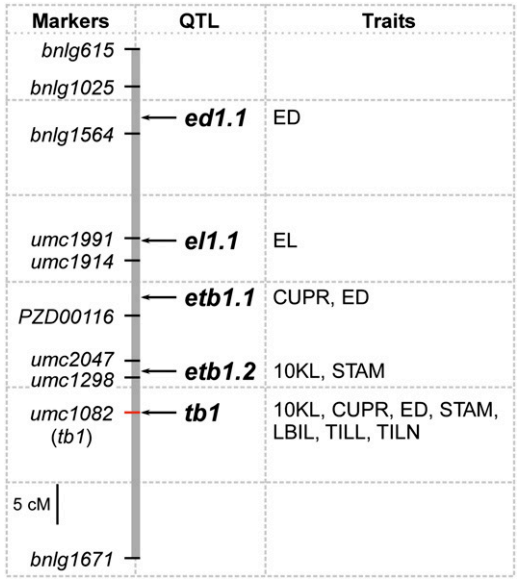

Figure 5 Map of the five QTL in our working model. Arrows indicate estimated positions of each QTL. Traits listed correspond to the phenotypes that map to each QTL. Flanking markers are included for reference. Traits are abbreviated as in Figure 2.

confirmed that *tb1* is a large effect QTL for seven of the eight traits analyzed (10KL, CUPR, ED, LBIL, STAM, TILL, and TILN). In particular, our results indicate that *tb1* is the only QTL for plant architecture traits including: LBIL, TILL, and TILN. These results are consistent with previous studies (Doebley *et al.* 1997; Clark *et al.* 2006). However, our analysis also detected several additional linked QTL located proximal to *tb1*, two of which interact epistatically with *tb1*. These additional QTL only affect ear traits (10KL, CUPR, ED, EL, and STAM).

Based on the results of experiments I and II, we proposed a model for the number and positions of QTL in the introgressed segment (Figure 5). This model assumes that *tb1* and its neighboring QTL have pleiotropic effects on multiple traits. From prior work, it is known that *tb1* has pleiotropic effects on 10KL, CUPR, LBIL, STAM, TILL, and TILN (Doebley *et al.* 1997; Clark *et al.* 2006). Our data confirm these observations as we detected pleiotropic effects of a QTL at *tb1* on all these traits as well as ED. Thus, we hypothesize that *tb1* is a QTL for seven traits (Figure 5). Our analyses reveal another QTL 14 cM proximal of *tb1* with effects on CUPR and ED, and which interacts epistatically with *tb1*. We designate this QTL *enhancer of tb1.1* (*etb1.1*). Our analyses also revealed another QTL 6 cM proximal of *tb1* with effects on 10KL and STAM, and which interacts epistatically with *tb1*. We designate this QTL *enhancer of tb1.2* (*etb1.2*). The epistatic interaction of *tb1* with both *etb1.1* and *etb1.2* is plainly visible in Figure 4. These results suggest the epistatic interaction between *tb1* and *etb1.2* (Figure 4, A and C) is stronger than the interaction between *tb1* and *etb1.1* (Figure 4, B and D). Two additional QTL exist in the introgressed segment: *ed1.1* and *el1.1*. These two QTL each affect a single trait (ED and EL, respectively) and neither shows an epistatic interaction with *tb1*. Together these five QTL explain the maize-like *vs.* teosinte-like phenotypes of the two parental lines (W22 and W22-T1L).

The data from Clark *et al.* (2006) also suggest the presence of additional QTL effecting CUPR downstream of *tb1*. For example, introgression lines containing the full teosinte introgressed segment (I01) have a strong effect on CUPR, while lines with the maize allele downstream of *tb1* have a weaker effect. An additional QTL downstream of *tb1* contributing to CUPR may be the reason that *cupr1.2* was not located directly over *tb1* in our experiment, but instead peaked distal to *tb1* (Figure 3). It is possible that our analysis did not identify a distal QTL because of its proximity to *tb1* and/or its effect size on CUPR.

Two QTL (*etb1.1* and *etb1.2*) identified in our experiments interact epistatically with *tb1* (Figure 4). Such epistatic interactions are generally difficult to detect in QTL mapping studies (Mackay *et al.* 2009), and thus the amount of epistasis detected in QTL mapping experiments varies from study to study (Flint and Mackay 2009). A QTL mapping experiment for flowering time in maize demonstrated that epistasis has a negligible effect on this trait, while other examples in the literature from Arabidopsis, flies, mice, and rice show large epistatic effects for various traits (Buckler *et al.* 2009; Flint and Mackay 2009).

There are at least two reasons that we were able to detect epistatic QTL. First, our experiments focused on a relatively small genomic region. Thus, we did not suffer the loss of statistical power that comes along with performing a large number of pairwise tests of epistasis as occurs with whole-genome scans for epistasis (Holland 2007). Second, the epistatic interactions detected in our analyses have relatively large effect sizes so that relatively little statistical power is needed to reject a false null hypothesis (Table 2). It may also be important that maize and teosinte diverged 10,000 generation ago and maintain separate gene pools and evolutionary trajectories. Thus, over time, maize and teosinte may have been selected for specific combinations of alleles at multiple loci, one combination adapted to natural conditions and the other to agricultural circumstances.

Both experiments I and II support the hypothesis that there are additional QTL linked to a major domestication locus (*tb1*). We detect these additional QTL in our teosinte × W22 mapping populations. It is unknown whether these QTL were involved in maize domestication or simply differentiate the maize inbred W22 and our specific teosinte parents. We do not know whether these QTL would have been detected had we used a different modern maize inbred or even a primitive maize variety. To address this possibility, we are currently attempting to clone *etb1.2*. Once the gene underlying *etb1.2* has been identified, we will have a critical tool for investigating its potential role in maize domestication and its interaction with *tb1*.

Acknowledgments

We thank Shawn Kaeppler for comments on this manuscript. This work was supported by the U. S. Department of Agriculture Hatch grant MSN101593 and the National Science Foundation grants DBI0321467 and DBI0820619.

Literature Cited

Broman, K. W., H. Wu, S. Sen, and G. A. Churchill, 2003 R/qtl: QTL mapping in experimental crosses. Bioinformatics 19: 889–890.

Buckler, E. S., J. B. Holland, P. J. Bradbury, C. Acharya, P. J. Brown *et al.*, 2009 The genetic architecture of maize flowering time. Science 325: 714–718.

Clark, R., T. Nussbaum-Wagler, P. Quijada, and J. Doebley, 2006 A distant upstream enhancer at the maize domestication gene, *tb1*, has pleiotropic effects on plant and inflorescence architecture. Nat. Genet. 38: 594–597.

Doebley, J., and A. Stec, 1991 Genetic analysis of the morphological differences between maize and teosinte. Genetics 129: 285–295.

Doebley, J., and A. Stec, 1993 Inheritance of the morphological differences between maize and teosinte: comparison of results for two F2 populations. Genetics 134: 559–570.

Doebley, J., A. Stec, and C. Gustus, 1995 *teosinte branched1* and the origin of maize: evidence for epistasis and the evolution of dominance. Genetics 141: 333–346.

Doebley, J., A. Stec, and L. Hubbard, 1997 The evolution of apical dominance in maize. Nature 386: 485–488.

Doerge, R. W., and G. A. Churchill, 1996 Permutation tests for multiple loci affecting a quantitative character. Genetics 142: 285–294.

Flint, J., and T. F. C. Mackay, 2009 Genetic architectures of quantitative traits in flies, mice and human. Genome Res. 19: 723–733.

Haley, C. S., and S. A. Knott, 1992 A simple regression method for mapping quantitative trait loci in line crosses using flanking markers. Heredity 69: 315–324.

Holland, J. B., 2007 Genetic architecture of complex traits in plants. Curr. Opin. Plant Biol. 10: 156–161.

Lander, E. S., and D. Botstein, 1989 Mapping Mendelian factors underlying quantitative traits using RFLP linkage maps. Genetics 121: 185–199.

Littel, R. C., G. A. Milliken, W. W. Stroup, and R. D. Wolfinger, 1996 *SAS System for Mixed Models*. SAS Institute, Cary, NC.

Mackay, T. F. C., E. A. Stone, and J. F. Ayroles, 2009 The genetics of quantitative traits: challenges and prospects. Nat. Rev. Genet. 10: 565–577.

Noor, M. A. F., A. L. Cunningham, and J. C. Larkin, 2001 Consequences of recombination rate variation on quantitative trait locus mapping studies: simulations based on the *Drosophila melanogaster* genome. Genetics 159: 581–588.

Communicating editor: A. Charcosset

GENETICS

Supporting Information
http://www.genetics.org/cgi/content/full/genetics.111.126508/DC1

Do Large Effect QTL Fractionate? A Case Study at the Maize Domestication QTL *teosinte branched1*

Anthony J. Studer and John F. Doebley

DOI: 10.1534/genetics.111.126508

Table S1 RFLP Markers used during backcrossing of T1L in Experiment II

Marker	Chromosome	Marker	Chromosome
bnl5.62	1	umc2a	3
umc157	1	php20725	4
umc37b	1	umc19	4
npi255	1	umc127a	4
BZ2	1	bnl10.17b	4
bnl8.10	1	umc15	4
npi615	1	bnl8.23	4
umc107	1	bnl8.33	5
npi225	1	bnl6.25	5
bnl8.45	2	umc90	5
umc53	2	umc27	5
npi320	2	umc166	5
npi421	2	bnl7.71	5
umc6	2	npi412	5
umc34	2	umc54	5
umc134	2	umc127b	5
umc131	2	umc104a	5
umc2b	2	bnl6.29	6
umc5a	2	umc65	6
php20005	2	umc21	6
umc122	2	umc46	6
umc49a	2	umc132	6
umc36	2	umc62	6
umc32	3	npi114	8
umc121	3	bnl9.11	8
php20042	3	umc117	8
umc42b	3	umc7	8
umc161	3	npi253	9
umc18	3	umc113	9
TE1	3	umc81	9
bnl5.37	3	umc95	9
bnl8.01	3	bnl3.04	10
umc60	3	umc130	10
bnl12.97	3	umc49b	10
php10080	3	umc117b	10
npi425	3	bnl7.49	10